

Evidence for an asteroid–comet continuum from simulations of carbonaceous microxenolith dynamical evolution

Giacomo BRIANI^{1,2,5*}, Alessandro MORBIDELLI³, Matthieu GOUNELLE², and David NESVORNÝ⁴

¹Dipartimento di Fisica e Astronomia, Università di Firenze, Largo E. Fermi 2, 50125 Firenze, Italy

²Laboratoire de Minéralogie et Cosmochimie du Muséum, UMR7202, Muséum National d'Histoire Naturelle – CNRS, 61 rue Buffon, 75005 Paris, France

³Département Cassiopée, UMR6202, Observatoire de la Côte d'Azur – CNRS, 06304 Nice Cedex 4, France

⁴Department of Space Studies, Southwest Research Institute, 1050 Walnut St., Suite 400, Boulder, Colorado 80302, USA

⁵Present address: Laboratoire Interuniversitaire des Systèmes Atmosphériques, UMR 7583 du CNRS, Universités Paris 7 et 12, Créteil, France

*Corresponding author. E-mail: giacomo.briani@lisa.u-pec.fr

(Received 16 March 2011; revision accepted 06 October 2011)

Abstract—Micrometeoroids with 100 and 200 μm size dominate the zodiacal cloud dust. Such samples can be studied as micrometeorites, after their passage through the Earth atmosphere, or as microxenoliths, i.e., submillimetric meteorite inclusions. Microxenoliths are samples of the zodiacal cloud dust present in the asteroid Main Belt hundreds of millions years ago. Carbonaceous microxenoliths represent the majority of observed microxenoliths. They have been studied in detail in howardites and H chondrites. We investigate the role of carbonaceous asteroids and Jupiter-family comets as carbonaceous microxenolith parent bodies. The probability of low velocity collisions of asteroidal and cometary micrometeoroids with selected asteroids is computed, starting from the micrometeoroid steady-state orbital distributions obtained by dynamical simulations. We selected possible parent bodies of howardites (Vesta) and H chondrites (Hebe, Flora, Eunomia, Koronis, Maria) as target asteroids. Estimates of the asteroidal and cometary micrometeoroid mass between 2 and 4 AU from the Sun are used to compute the micrometeoroid mass influx on each target. The results show that all the target asteroids (except Koronis) receive the same amount (within the uncertainties) of asteroidal and cometary micrometeoroids. Therefore, both these populations should be observed among howardite and H chondrite carbonaceous microxenoliths. However, this is not the case: carbonaceous microxenoliths show differences similar to those existing among different groups of carbonaceous chondrites (e.g., CI, CM, CR) but two sharply distinct populations are not observed. Our results and the observations can be reconciled assuming the existence of a continuum of mineralogical and chemical properties between carbonaceous asteroids and comets.

INTRODUCTION

The inner solar system is pervaded by a population of small objects, from submicrometer-sized dust grains to centimeter-sized meteoroids, that form the zodiacal cloud, visible in a clear night sky as the zodiacal light. Forces such as the gravity of the Sun and the planets, the radiation pressure, the Poynting–Robertson effect, the solar wind drag as well as mutual collisions act to shape the zodiacal cloud (Gustafson 1994). Direct

measurements from satellite (performed by the Long Duration Exposure Facility; Love and Brownlee 1993) and models based on lunar cratering and on measurements of the Pioneer spacecraft (Grün et al. 1985) showed that at 1 AU from the Sun the zodiacal cloud mass distribution is dominated by micrometeoroids with a size of 200 μm . Micrometeoroids with size $\geq 100 \mu\text{m}$ have a lifetime; determined by collisions (Leinert et al. 1983), which fragment them in smaller dust particles in approximately 5×10^5 yr (Grün et al. 1985;

Nesvorný et al. 2010). Therefore, to maintain the observed steady state of the zodiacal cloud, it is necessary that larger bodies act as sources of micrometeoroids. Such bodies are asteroids and comets. Micrometeoroids can derive from asteroids and comets via collisional cascade processes and comets, in addition, expulse micrometeoroid-sized fragments when they are active.

There are two possibilities to study in our laboratories the micrometeoroids that dominate the zodiacal cloud: the first is represented by micrometeorites (and, for the lowest tail of the size distribution, by interplanetary dust particles); the second by microxenoliths, i.e., inclusions that have an origin different from that of their host meteorites.

Micrometeorites have been recovered from different places: deep sea sediments, sedimentary rocks, Greenland ice-caps, and Antarctica (Taylor and Brownlee 1991; Engrand and Maurette 1998; Duprat et al. 2007). The great abundance of micrometeorites recovered from Antarctica in the last years allowed an extended and in-depth study of their composition, petrography, and mineralogy (see, e.g., Genge et al. 2008; Dobricá et al. 2009). About 84% of micrometeorites are samples of carbonaceous material, with the other 16% being associated with ordinary chondrites (Genge 2006), while very rare are basaltic micrometeorites (Gounelle et al. 2009).

A complicated issue concerning micrometeorites is that of identifying their parent bodies. Several arguments have been presented to support both the hypothesis that micrometeorites originate from asteroids (see, e.g., Flynn 1995; Levison et al. 2009) and the hypothesis that they come from comets (Maurette et al. 2000; Duprat et al. 2010; Nesvorný et al. 2010). Indeed, due to their smaller dimensions, the dynamical evolution of micrometeorites toward the Earth is different from that of larger meteorites (Gustafson 1994). This leads (1) to the idea that micrometeorites represent a more uniform sampling of the whole asteroid Main Belt than meteorites (Genge et al. 1997; Meibom and Clark 1999), and (2) to the possibility that cometary micrometeorites arrive at the Earth on orbits reminiscent of those of asteroidal particles (Nesvorný et al. 2010). This complicates the task of identifying the micrometeorite parent bodies.

Microxenoliths are commonly observed in meteorites (Wilkening 1977; Lipschutz et al. 1989; Bischoff et al. 2006). The most abundant microxenoliths are those that present mineralogical and petrographic properties similar to those of carbonaceous chondrites (Wilkening 1977; Lipschutz et al. 1989; Meibom and Clark 1999; Bischoff et al. 2006; Rubin and Bottke 2009). A detailed study has been realized for howardite microxenoliths (Gounelle et al. 2003, 2005). In a companion paper (Briani et al.

Forthcoming), we describe a systematic analysis of carbonaceous microxenoliths in H chondrites.

Even if both micrometeorites and microxenoliths derive from zodiacal cloud micrometeoroids, microxenoliths have peculiar properties that make them unique samples. First, microxenoliths can be considered as fossil micrometeorites. The Earth geological activity destroys micrometeorites in relatively short time periods. Micrometeorites and cosmic spherules (totally melted micrometeorites) recovered on the Earth show maximum ages of about 470 Myr (Meier et al. 2010). Instead microxenoliths represent samples of the zodiacal dust population over a time span much longer than that sampled by micrometeorites. This is supported by the observation that asteroids and comets have no important geological activity, and therefore present favorable conditions to preserve microxenoliths for long periods of time. Also, we note that howardites and most of the H chondrites that contain microxenoliths are regolith breccias, i.e., they formed from the compaction of regolith layers on the parent body surfaces. Calculations based on asteroid absolute magnitudes, colors, and ages show that the gardening time scale (i.e., the time needed to refresh an evolved surface) is ~ 4.4 Gyr (Willman and Jedicke 2011). Given these long time scales of regolith evolution, microxenoliths have had the possibility of residing undisturbed on the asteroid surfaces for hundreds of millions years. Second, microxenoliths sample the zodiacal cloud at distances corresponding to those of the asteroid Main Belt, i.e., between 2 and 4 AU, whereas micrometeorites are samples of the zodiacal cloud at 1 AU.

Here, we present a study on the possible parent bodies of carbonaceous microxenoliths. We focused on two classes of minor bodies that can produce carbonaceous micrometeoroids: Jupiter-family comets (JFCs) and primordial asteroids (C-, D-, and P-type asteroids). Assuming that microxenoliths are intact micrometeoroids embedded in the meteorite parent bodies we performed dynamical simulations to evaluate the micrometeoroid flux on selected target asteroids, supposed to be the parent bodies of the meteorites in which carbonaceous microxenoliths have been observed. To perform such a calculation, we assume that the observed microxenoliths are representative of the current steady state of dust crossing the asteroid belt. As microxenoliths can be very ancient samples, this may not be appropriate, in principle. We elaborate on the validity of this assumption in the Discussion section.

Our aim is to compare the microxenolith contributions of primordial asteroids and JFCs with the microxenolith populations observed in howardites and H chondrites. This will help to understand if it is possible to positively distinguish cometary and asteroidal samples among

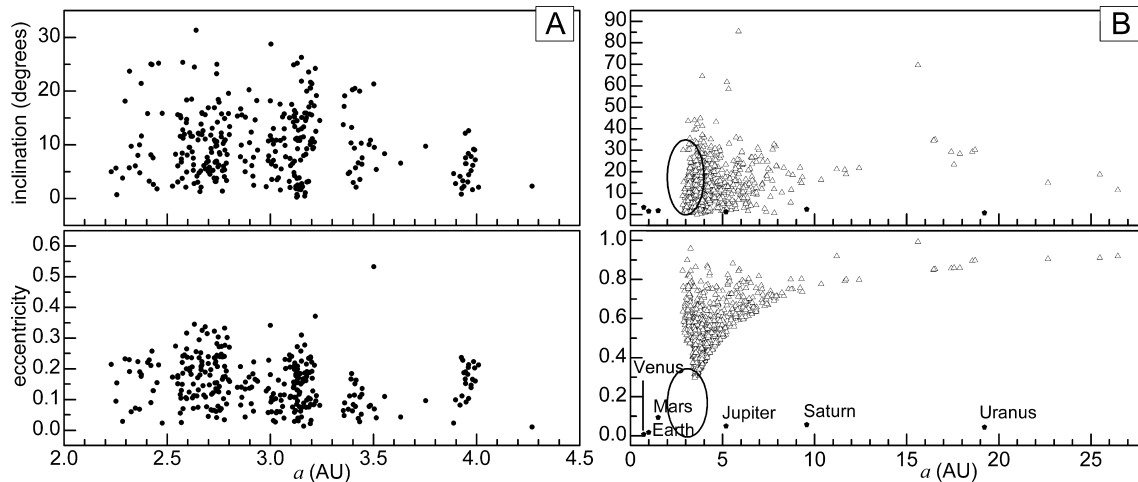


Fig. 1. Semimajor axis (a) versus eccentricity (bottom row) and inclination (top row) of the initial populations (1000 particles each) of micrometeoroids originated from C-, D-, and P-type asteroids (A) and of micrometeoroids originated from Jupiter-family comets (B). Note the different scales of the horizontal axis in (A) and (B). The two ellipses in (B) indicate the regions corresponding to the initial conditions of asteroidal micrometeoroids shown in (A). The orbital elements of six planets—Venus to Uranus—are shown in (B) for reference.

microxenoliths or if, instead, the observed microxenoliths support the idea of a continuum between carbonaceous asteroids and comets.

MODEL INPUTS

Here, we report the assumptions that we made and previous results on which we rely to perform our simulations. All this is justified in more detail in the Discussion section.

Microxenoliths Parent Bodies

Given that among observed microxenoliths the vast majority is represented by carbonaceous materials, as possible microxenolith parent bodies we focus on primordial asteroids and JFCs. As primordial asteroids we consider here the asteroids of spectral type C, D, and P (following the Tholen classification; Tholen 1989). JFCs have been recently proposed as the most important sources of present-day zodiacal cloud particles and of carbonaceous micrometeorites (Nesvorný et al. 2010).

Micrometeoroid Initial Conditions

To compute the micrometeoroid flux on the selected target asteroids we started from two populations, each of 1000 particles, representative of JFC and asteroidal micrometeoroids.

The initial orbital distribution of JFC micrometeoroids has been prepared starting from the orbital elements of

JFCs that have perihelion $q < 2.5$ AU for the first time (i.e., the JFCs that become active and produce important amount of micrometeoroids). Indeed, we considered 1000 synthetic JFC orbits, extracted from simulations for the Kuiper Belt contribution to the JFC population (Levison and Duncan 1997). Each of the 1000 JFC orbits has been considered as the initial orbit of a micrometeoroid.

For the initial orbital distribution of asteroidal micrometeoroids, we selected the orbital elements of 310 C-, D-, and P-type asteroids, as listed in the JPL Small Body Database (<http://ssd.jpl.nasa.gov/sbdb.cgi>). In choosing the 310 asteroids, no limits have been imposed on their size or on their magnitude. To obtain the initial orbits of 1000 micrometeoroids, we cloned the 310 asteroidal orbits varying the mean anomaly M : for each original orbit, three or four more orbits have been obtained uniformly varying M over 360° . Initial semimajor axis, eccentricity, and inclination of these two populations of micrometeoroids are reported in Fig. 1.

Target Asteroids

We selected as targets those asteroids that have been proposed as parent bodies of howardites, i.e., 4 Vesta (Binzel and Xu 1993; Drake 2001), and of H chondrites: 6 Hebe, 8 Flora, 15 Eunomia, 158 Koronis, and 170 Maria (Farinella et al. 1993; Migliorini et al. 1997; Gaffey and Gilbert 1998; Rubin and Bottke 2009). Their orbital inclinations and eccentricities are shown in Fig. 2. In Table 1 are reported the complete orbital properties of the six selected target asteroids.

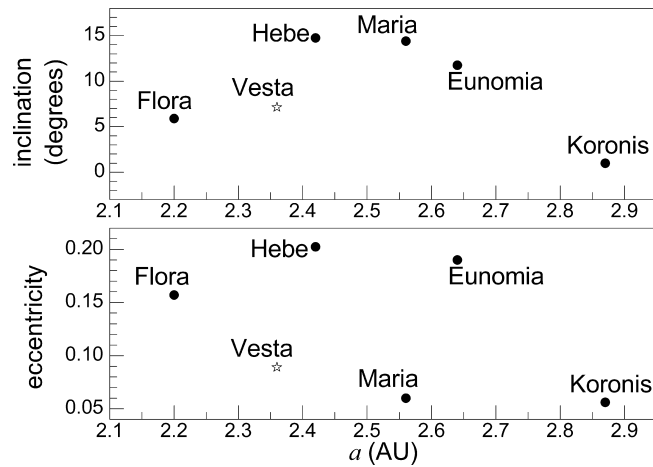


Fig. 2. Semimajor axis (a), eccentricity, and inclination of the six asteroids selected as targets in our simulations. Black dots indicate possible parent bodies of H chondrites. Vesta, parent body of howardites, has a different symbol.

Table 1. Orbital properties of the six asteroids selected as targets in our simulations.

Asteroid	a (AU)	e	i (°)	Ω (°)	ω (°)	M (°)
4 Vesta	2.36	0.09	7.13	103.9	149.8	307.8
6 Hebe	2.42	0.20	14.8	138.7	239.5	331.8
8 Flora	2.20	0.16	5.89	111.0	285.2	309.3
15 Eunomia	2.64	0.19	11.7	293.2	97.8	270.2
158 Koronis	2.87	0.055	1.00	278.4	141.7	289.5
170 Maria	2.55	0.062	14.4	301.4	157.7	278.1

Notes: Data are from the JPL Small Body Database (<http://ssd.jpl.nasa.gov/sbdb.cgi>). a = semimajor axis; e = eccentricity; i = inclination; Ω = longitude of the ascending node; ω = argument of periapsis; M = mean anomaly.

Micrometeoroids–Asteroids Collision Velocity

We assume that microxenoliths are really embedded micrometeoroids and not fragments of larger bodies produced in the impact with the host meteorite. This requires that micrometeoroids collide with the target asteroids at low velocity, such that they can avoid strong shock effects. Here, we do not treat in detail the problem of low velocity collisions, but we assume a value of 1.5 km s^{-1} as velocity below which micrometeoroids are unaffected by the collisions. This means that, for the evaluation of the probability of impact between micrometeoroids and target asteroids, we do not take into account those micrometeoroids that collide at speed $> 1.5 \text{ km s}^{-1}$.

The collision velocity is calculated taking into account the gravitational focusing of the target asteroids, as described in more detail in the Appendix.

Micrometeoroid Mass Between 2 and 4 AU

Nesvorný et al. (2010) estimate that the total mass of the zodiacal cloud (within 5 AU from the Sun) is $5.2 \times 10^{19} \text{ g}$, 15% of which is due to asteroidal micrometeoroids and the rest to cometary micrometeoroids. This value is obtained considering spherical particles with diameter $200 \mu\text{m}$ and density 2 g cm^{-3} as the most abundant zodiacal cloud components. The total mass estimate is uncertain by a factor of approximately 2, because it depends on the assumed size and density of the zodiacal cloud particles. Concerning the micrometeoroid radial distribution, Nesvorný et al. (2010) report that approximately 30% of JFC particles, equivalent to $1.6 \times 10^{19} \text{ g}$, is within 4 AU from the Sun, and that approximately 10% ($5.2 \times 10^{18} \text{ g}$) is within 2 AU. For asteroidal particles, the mass within 4 AU from the Sun is $1.3 \times 10^{18} \text{ g}$, that within 2 AU $5.3 \times 10^{17} \text{ g}$. Thus, the total mass of cometary micrometeoroids between 2 and 4 AU is $1.08 \times 10^{19} \text{ g}$ and that of asteroidal micrometeoroids is $7.7 \times 10^{17} \text{ g}$.

However, we do not use this total value of the asteroidal micrometeoroid mass, because part of this mass is due to noncarbonaceous micrometeoroids. As possible micrometeoroid parent bodies we selected C-, D-, and P-type asteroids on the basis of the Tholen spectral classification (Tholen 1989). In Bus et al. (2002), there is a table with the equivalence between the asteroidal spectral classes of the Tholen and of the SMASS II asteroid classification. Data for the number of asteroids in the different SMASS II spectral classes are present in Bus and Binzel (2002). Based on these references, we assume the value 0.41 as the fraction of C-, D-, and P-type asteroids and hence of carbonaceous micrometeoroids. This gives, between 2 and 4 AU, a carbonaceous micrometeoroid mass of $3.16 \times 10^{17} \text{ g}$, and therefore a cometary to asteroidal mass ratio $R = 34$.

NUMERICAL SIMULATIONS

To estimate the collision probability of micrometeoroids with the target asteroids, we need to know the steady-state orbital distribution of asteroidal and cometary micrometeoroids. For this, we performed numerical simulations of their orbital evolution, assuming a micrometeoroid density of 2 g cm^{-3} and a micrometeoroid diameter of $200 \mu\text{m}$. Numerical simulations have been performed with the `swift_rmvs3_pr` code (Nesvorný et al. 2006). The code integrates the orbits of massless particles under the action of gravity of the Sun and seven planets (Venus to Neptune), radiation pressure, solar wind, and Poynting-Robertson drag. The numerical integration of a particle orbit is stopped if that particle collides with a planet or if it is ejected from the solar

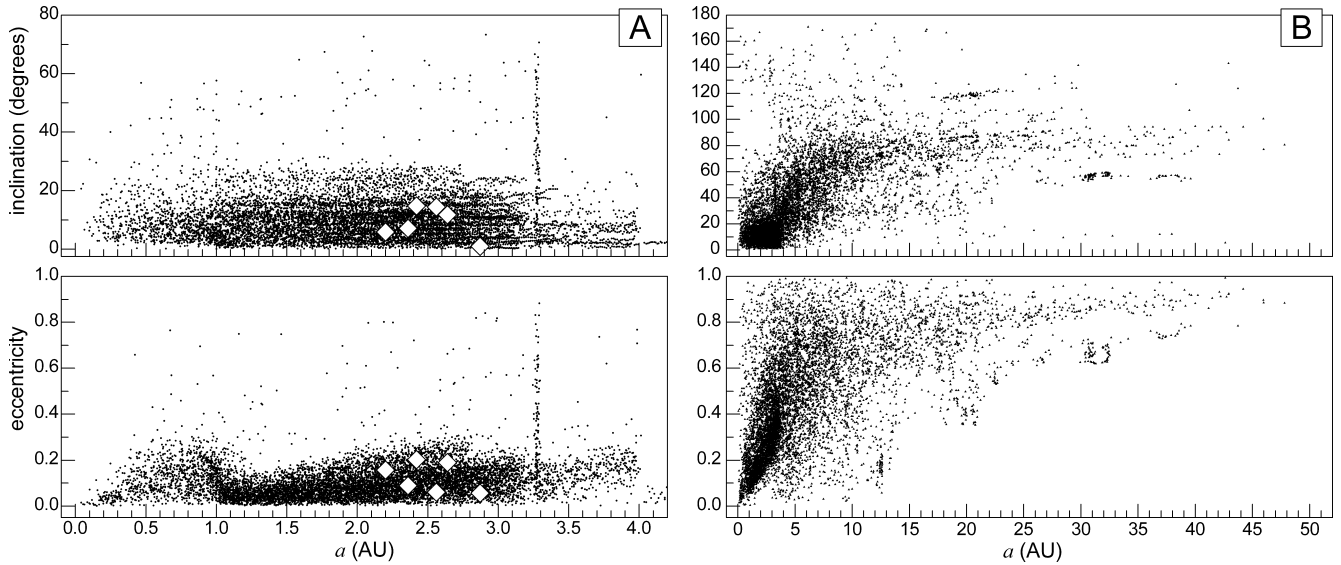


Fig. 3. Semimajor axis (a) eccentricity and inclination of the steady-state orbital distribution of asteroidal (A) and Jupiter-family comet (B) micrometeoroids (for clarity, only 10% of the considered orbits are reported in the figure). White diamonds in panel (A) represent the six target asteroids. In the steady-state orbital distribution of asteroidal micrometeoroids, the effect of several mean motion resonances is evident, in particular at $a = 3.28$ AU (the Jupiter 2:1 mean motion resonance) and $a = 1$ AU (the Earth 1:1 mean motion resonance).

system or if it drifts to within 0.04 AU. We set 0.04 AU as inferior limit to the particle distance from the Sun because it is very unlikely that particles within 0.04 AU from the Sun are scattered back into the 2–4 AU region (where our target asteroids are) by encounters with the terrestrial planets. Therefore, we can suppress these particles without altering the population statistics in our region of interest. We set the duration of our simulations to 10 Myr, a period after which almost all the orbit integrations have been stopped. The collection of all the simulated orbits over the period of 10 Myr is assumed as representative of the steady-state orbital distribution of micrometeoroids (Fig. 3).

Once the steady-state orbital distributions of asteroidal and cometary micrometeoroids are obtained, it is possible to calculate the amount of mass that each of these two populations delivers to the target asteroids. To do this, we take advantage of the fact that all target asteroids are between 2 and 4 AU and that we have an independent mass estimate of the amount of asteroidal and cometary micrometeoroids in the 2–4 AU annulus from the work of Nesvorný et al. (2010). Thus, we consider only the micrometeoroid orbits that intersect the 2–4 AU annulus and, for each orbit j ($j = 1 \dots N$), we compute the fraction F_j that is contained in this annulus. Once selected a target asteroid, the intrinsic collision probability p_j between the micrometeoroid and the target is calculated following the Wetherill (1967) algorithm. This algorithm, given the semimajor axis a , eccentricity e , and inclination i of the two orbits, assumes

that the angles M , ω , Ω (mean anomaly, argument of perihelion, and longitude of the ascending node) of the micrometeoroid and the target have a uniform probability distribution over the range $0-2\pi$; then it computes which fraction of these angles corresponds to the two objects being closer to each other than 1 km; finally, this fraction is translated into a collision probability per year (p_j), using the orbital periods of the two objects and assuming that they are not in resonance with each other. As we are interested only in collisions that can produce unshocked microxenoliths, we modified this algorithm to take into account only orbital intersections corresponding to relative speeds smaller than 1.5 km s^{-1} . Once all p_j computed, the micrometeoroid mean collision probability with the target is computed as

$$p_{\text{coll}} = \frac{\sum_{j=1}^N p_j}{\sum_{j=1}^N F_j}. \quad (1)$$

Finally, this allows us to compute the ratio of cometary to asteroidal micrometeoroid flux for each target as

$$\varphi = \frac{p_{\text{coll}}^{\text{JFC}}}{p_{\text{coll}}^{\text{AST}}} \times R, \quad (2)$$

where $R = 34$ is the cometary to asteroidal micrometeoroid mass ratio in the 2–4 AU annulus.

Table 2. Mean collision probability and mean collision velocity of asteroidal and Jupiter-family comet micrometeoroids for each of the considered targets (only micrometeoroids colliding with impact speed $< 1.5 \text{ km s}^{-1}$ are considered).

Source	Target	Mean collision probability ($\times 10^{-21} \text{ km}^{-2} \text{ yr}^{-1}$)	Mean collision velocity (m s^{-1})
C-, D-, P-type asteroids	4 Vesta	89 ± 3	416 ± 5
	6 Hebe	7.5 ± 0.2	167 ± 10
	8 Flora	24.1 ± 0.7	255 ± 6
	15 Eunomia	4.9 ± 0.1	198 ± 8
	158 Koronis	211 ± 7	1135 ± 4
	170 Maria	36 ± 1	101 ± 0.6
Jupiter-family comets	4 Vesta	2.0 ± 0.7	410 ± 5
	6 Hebe	1.6 ± 0.7	167 ± 10
	8 Flora	4.2 ± 0.7	273 ± 5
	15 Eunomia	1.3 ± 0.4	202 ± 8
	158 Koronis	0.2 ± 0.4	985 ± 4
	170 Maria	0.5 ± 0.4	83 ± 0.6

RESULTS

The values of the mean collision probability and of the mean collision velocity of asteroidal and JFC micrometeoroids for each considered target are reported in Table 2. Using Equation 2, we obtained the cometary to asteroidal micrometeoroid flux ratio φ for each selected target asteroid: our results are shown in Fig. 4. In this figure, error bars correspond to uncertainties estimated as reported in the Appendix (Equation A6). They are calculated from the uncertainties on the cometary to asteroidal micrometeoroid mass ratio between 2 and 4 AU (Nesvorný et al. 2010) and on the mean collision probability. In particular, to evaluate the uncertainty on p_{coll} we took into account both the uncertainty due to our numerical simulations and that due to the fact that micrometeoroids with different physical properties (in particular size and density) follow different orbital evolutions (see Appendix for the details).

Results in Table 2 show that the mean collision velocity between micrometeoroids and target asteroids are very low. We point out again that such values are calculated without considering collisions for which the impact speed is $> 1.5 \text{ km s}^{-1}$. However, collisions selected with such a threshold happen on average at very low speed, always less than about 400 m s^{-1} (except for Koronis). This makes us confident that such impacts can produce unshocked microxenoliths as those observed in howardites (Gounelle et al. 2003) and H chondrites (Briani et al. Forthcoming).

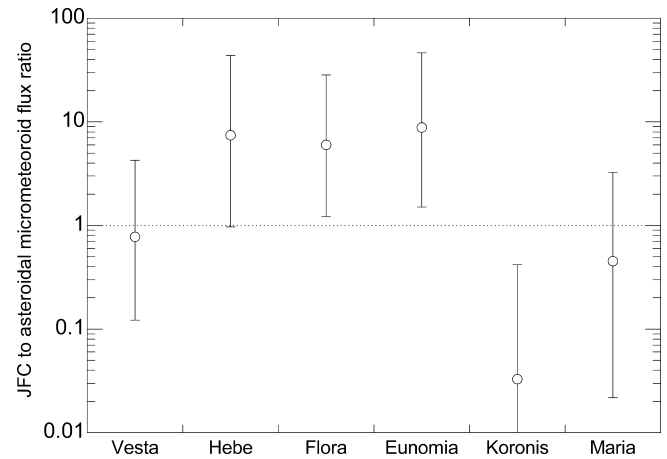


Fig. 4. Jupiter-family comet to asteroidal micrometeoroid flux ratio for the six target asteroids considered in this work. Error bars correspond to the uncertainties calculated as shown in the Appendix.

Our results (Fig. 4) show that for Vesta, Hebe, and Maria the value of φ is consistent with 1 (within the estimated uncertainty), for Flora and Eunomia the flux of JFC micrometeoroids is slightly larger than the flux of asteroidal micrometeoroids ($\varphi > 1$), while Koronis is the only target asteroid for which the flux of asteroidal micrometeoroids is clearly larger than the flux of JFC micrometeoroids ($\varphi < 1$).

These results indicate that in howardites, as they originate from Vesta, two populations of microxenoliths, cometary and asteroidal, should be present. The same is true for H chondrites if they originate from Hebe and/or Maria. Instead, if H chondrites originate from Flora and/or Eunomia, then cometary microxenoliths should be more abundant, while if Koronis is the H chondrite parent body, then asteroidal microxenoliths prevail.

DISCUSSION

In our simulations, we focused on the orbital evolution of particles that are possible precursors of carbonaceous microxenoliths because these represent the vast majority of microxenoliths in both howardites and H chondrites. The general mineralogical and petrographic properties of carbonaceous microxenoliths are similar in both howardites and H chondrites, indicating that these samples belong to the same class of extraterrestrial objects. They are dominated by a fine-grained matrix, mainly composed of submicrometric grains of phyllosilicates, which supports different amounts of larger anhydrous silicates, carbonates, sulfides, magnetite, and metal grains. Carbonaceous microxenoliths can be classified in different groups on the basis of their petrography and mineralogy (Gounelle

et al. 2003). Indeed, carbonaceous microxenoliths are usually compared to CI, CM, and CR chondrites (Greshake et al. 2002; Gounelle et al. 2003; Nakashima et al. 2003; Briani et al. Forthcoming).

The asteroids of spectral type C, D, and P are usually supposed to be the parent bodies of carbonaceous chondrites. In particular, C-type asteroids have reflectance spectra similar to those of CM and CI carbonaceous chondrites, characterized by the presence of an absorption band near 3 μm due to hydrated silicates (Johnson and Fanale 1973; Vilas and Gaffey 1989; Hiroi et al. 1993a, 1993b), while reflectance spectra of D- and P-type asteroids, which do not show the 3 μm absorption band, have been linked to chondritic porous IDPs (Bradley et al. 1996). We did not consider S-type asteroids as possible microxenolith parent bodies because their spectroscopic signatures suggest links with ordinary chondrites, but not with carbonaceous materials (Burbine et al. 2002).

Jupiter-family comets appear to be the main sources of submillimetric zodiacal cloud particles (Nesvorný et al. 2010). However, the contribution of primordial asteroids to the microxenolith population can be as important, because we consider targets in the asteroid Main Belt, i.e., the same place where asteroidal micrometeoroids are produced.

Among the target asteroids, we selected Vesta because it is usually considered the parent body of howardites: its reflectance spectrum is similar to those of howardites (and eucrites) and Vesta fragments (asteroids < 10 km in size) have been observed between the ν_6 secular resonance and the 3:1 mean motion resonance with Jupiter (at 2.5 AU), attesting that meteoroids from Vesta could have been transported into Earth crossing orbits (Binzel and Xu 1993; Drake 2001).

Hebe was proposed as a possible parent body of H chondrites, because its fragments can be driven to the Earth by the ν_6 secular resonance or the 3:1 mean motion resonance with Jupiter (Migliorini et al. 1997; Gaffey and Gilbert 1998), and because its reflectance spectra are consistent with those of H chondrites (Farinella et al. 1993). More recent studies have highlighted that Hebe is not likely the parent body of H chondrites and that ordinary chondrites (i.e., H, L, LL chondrites) more probably derive from the Flora, Eunomia, Koronis, and Maria asteroid families (see Rubin and Bottke (2009) for a critical and detailed discussion). However, Bottke et al. (2010) argued once again that Hebe is the real H chondrite parent body because: (1) the Ar-Ar shock degassing ages of H chondrites range from today to 4.5 Ga, without evidence of a family-forming event; (2) the H chondrites cosmic ray-exposure age distribution shows a peak around 7–8 Myr that can be explained as due to impact with

fragments generated by the Veritas family-forming event; and (3) a new model to study the origin of meteorites shows that three out of six H chondrites with known orbits come from the 3:1 mean motion resonance, and the other three come from the ν_6 secular resonance, both path being consistent with the Hebe location. In conclusion, the parent body of H chondrites is not known with confidence, and therefore we included several asteroids in our target list. In particular, Rubin and Bottke (2009) suggest the Flora, Eunomia, Koronis, and Maria asteroid families as possible H chondrite parent bodies. We therefore selected as targets the four asteroids from which these families take their names.

The absence of evident shock effects in microxenoliths and the differences with respect to larger carbonaceous xenoliths found in the same groups of meteorites (Zolensky et al. 1996; Briani et al. Forthcoming) suggest that they are not fragments of larger bodies disrupted in violent impacts. Rather microxenoliths are micrometeoroids embedded at low velocity in their host meteorites. Laboratory experiments have shown that for an impact speed of 1.8 km s^{-1} , ordinary chondritic projectiles launched in quartz sand produce intact fragments that have up to 3.7% of the projectile mass (Bland et al. 2001). In these experiments, for impact speeds between 1.4 and 1.8 km s^{-1} , the largest fragments recovered have a dimension of several hundred micrometers, i.e., those of microxenoliths observed in howardites and H chondrites. However, carbonaceous material has probably lower strength than ordinary chondritic material. Indeed, Gounelle et al. (2003), performing numerical simulations similar to those presented here, assumed 1 km s^{-1} as maximum velocity to avoid alterations caused by the increase of temperature and shocks. In Chappelow and Sharpton (2006), the adopted value is 1.5 km s^{-1} . A more conservative value, 300 m s^{-1} , is indicated in Rubin and Bottke (2009). Clearly the maximum value of speed at which significant alterations are avoided strongly depends on the projectile and target properties and also on the angle of impact.

The effects of mutual disruptive collisions between micrometeoroids are neglected in our simulations. This may affect the results, in principle, but it is done because accounting for the full collisional cascade of the dust particles is very complicated in the dynamical simulations. Nesvorný et al. (2010) showed that, for modeling IRAS observations of the zodiacal cloud, collisional disruptions can be neglected as long as the collisional lifetime is longer than 5×10^5 yr, which is the case for particles larger than 100 μm in diameter. This gives us confidence that neglecting collisional disruption is an appropriate approximation also in our case.

To evaluate the uncertainties on our collision probabilities of dust particles with a target asteroid, we

also performed simulations for micrometeoroids with diameter 100 μm . The relative differences of collision probability between the case of 200 μm particles and the case of 100 μm particles are between 1% and 3% for asteroidal micrometeoroids, whereas for JFC micrometeoroids these differences are as follows: 34% for Vesta, 45% for Hebe, 16% for Flora, 29% for Eunomia, 215% for Koronis, and 77% for Maria. The absolute differences between collision probabilities are used to estimate the uncertainties on our collision probabilities as described in the Appendix (Equation A3). We chose the simulations for 200 μm diameter micrometeoroids as the reference simulations because in this way we can use the Nesvorný et al. (2010) zodiacal cloud mass estimations to calibrate our results.

Our results have been obtained assuming that the fraction of micrometeoroids originated from primordial asteroids is equal to the fraction of C-, D-, and P-type asteroids in the Main Belt (fraction estimated on the basis of the Tholen classification). However, Tomeoka et al. (2003) and Flynn et al. (2009) showed that, under the effect of hypervelocity impacts, hydrous asteroids produce larger amounts of micrometeoroid-sized fragments than anhydrous asteroids. Therefore, among asteroidal micrometeoroids the fraction of the hydrous ones is probably larger than the fraction of C-, D-, and P-type asteroids (41%) that we assumed. Indeed we are interested in hydrous micrometeoroids, because carbonaceous microxenoliths in both howardites and H chondrites are dominated by a fine-grained, hydrous matrix. Changing the fraction of micrometeoroids originated from primordial asteroids implies a small but important change in our results. If we assume that the fraction of carbonaceous asteroidal micrometeoroids is 50% of the mass reported in Nesvorný et al. (2010), then our results (Fig. 5) show that also for Flora the JFC to asteroidal micrometeoroid flux ratio is consistent with 1 (within the uncertainties). And if the fraction of carbonaceous asteroidal micrometeoroids is as high as 65% of the mass reported in Nesvorný et al. (2010), then also for Eunomia the JFC to asteroidal micrometeoroid flux ratio is consistent with 1 (Fig. 5). This implies that all the possible H chondrite parent bodies considered in present work, with the only exception of Koronis, can receive similar amount of JFC and asteroidal micrometeoroids, and therefore that H chondrites should contain both cometary and asteroidal microxenoliths, as it ought to be for howardites.

IMPLICATIONS

We compare here our results to the observed populations of carbonaceous microxenoliths in howardites and H chondrites. For the sake of reasoning, we assume

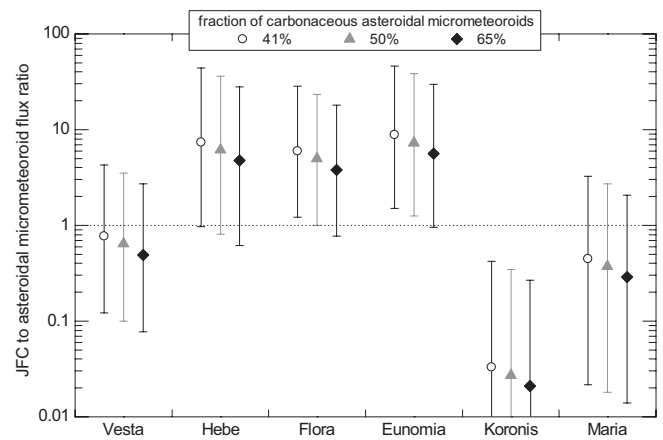


Fig. 5. Jupiter-family comet to asteroidal micrometeoroid flux ratio for the six target asteroids considered in this work. As part of asteroidal micrometeoroids derives from noncarbonaceous asteroids, we estimated this ratio assuming different values of the fraction of asteroidal carbonaceous micrometeoroids.

that primordial asteroids and comets are sharply different bodies.

If one considers the error bars on the results for Vesta, Fig. 5 shows that Vesta receives at least approximately 10% of cometary micrometeoroids. However, if such a fraction of cometary microxenoliths, clearly distinct from asteroidal microxenoliths, was present in howardites, then these two populations would have been observed, while they are not (Gounelle et al. 2003, 2005). Figure 5 also shows that, if the H chondrites originate from Hebe, Flora, or Eunomia, it is possible that the majority of H chondrite microxenoliths are cometary and hence different from howardite microxenoliths. However, radical differences between H chondrite microxenoliths (Briani et al. Forthcoming) and howardite microxenoliths are not observed.

Our simulations show that the considered target asteroids (with the exception of Koronis) receive similar fluxes of micrometeoroids originated from primordial asteroids and of micrometeoroids originated from JFCs. Therefore, two distinct groups of carbonaceous microxenoliths, asteroidal and cometary, should be observed in the meteorites originated from these asteroids. However, this is not the case. Certainly, carbonaceous microxenoliths observed in both howardites (Gounelle et al. 2003, 2005) and in H chondrites (Briani et al. Forthcoming) present petrographic and mineralogical differences, such that they can be classified in different groups (usually on the basis of similarities with carbonaceous chondrite groups), but not sufficient to justify the hypothesis of two radically distinct classes of parent bodies.

The hypothesis that primordial asteroids and comets are sharply different implies that asteroidal and cometary micrometeoroids have different structure. This means, in particular, that they have different mechanical strength

and therefore different abilities to survive impacts with a target asteroid. If cometary micrometeoroids are mostly similar to cluster IDPs, i.e., porous aggregates of small grains, then they have a significantly lower mechanical strength than more compact, asteroidal micrometeoroids. This would imply that the vast majority of microxenoliths are of asteroidal origin and this would explain why two sharply different populations of microxenoliths are not observed in howardites and H chondrites. Indeed, for certain cometary particles (namely the Draconid meteoroids) a very low density (0.3 g cm^{-3}) and high porosity (90%) have been deduced from observations, corresponding to a mechanical strength of 5–20 kPa (Borovička et al. 2007). However, other stream meteoroid families (associated with cometary parent bodies) show higher mean density, between 0.4 and 2.9 g cm^{-3} (Borovička 2006; Babadzhanov and Kokhirova 2009). In addition the meteoroid mineralogical density, i.e., the density of the constituent grains, is even higher, with values ranging between 2.25 and 3.4 g cm^{-3} (Babadzhanov and Kokhirova 2009). Such constituent grains have mechanical strength up to 2 MPa (Borovička 2006). They have mean sizes between 40 and $110 \mu\text{m}$, i.e., the same order of magnitude of carbonaceous microxenoliths, while the observed stream meteoroids have sizes $> 1 \text{ mm}$. Therefore, a density of 2 g cm^{-3} , as assumed in this work, is not unrealistic for cometary micrometeoroids, and we can safely assume the same mechanical strength for asteroidal and cometary micrometeoroids.

All these considerations do not validate the hypothesis that there exist strong differences between microxenolith parent bodies, as those that are usually supposed to exist between asteroids and comets.

Comets and asteroids (even primordial asteroids) are usually supposed to have different properties (e.g., composition, mineralogy, density) that reflect their different histories. Comets formed in the cold outer solar system are expected to be rich in ices and not to have suffered secondary processes like aqueous alteration and thermal metamorphism (see, e.g., Cottin et al. 1999; Brownlee 2003), which instead have been essential for asteroidal material (Brearley 2006; see, e.g., Huss et al. 2006). With this template in mind, the most unaltered extraterrestrial samples have been supposed to be associated with comets. For instance, a cometary origin has been proposed for chondritic porous IDPs (Bradley 2003), which do not contain minerals formed by aqueous alteration and are rich in carbonaceous material. Isotopic properties also support the idea that some IDPs and micrometeorites come from comets. Indeed certain comets (e.g., 17P/Holmes and Hale-Bopp) show a nitrogen isotopic composition enriched in ^{15}N (Manfroid et al. 2005; Bockelée-Morvan et al. 2008), and similar values of the $^{15}\text{N}/^{14}\text{N}$ ratio have been observed in some

IDPs (Floss et al. 2006). Also, elevated D/H ratios are observed in long-period comets (Balsiger et al. 1995; Eberhardt et al. 1995; Bockelée-Morvan et al. 1998; Meier et al. 1998). Duprat et al. (2010) described micrometeorites with very high content of organic matter (up to 85% of the analyzed surface for a single micrometeorite), which show very elevated D/H ratios (up to $[4.6 \pm 0.5] \times 10^{-3}$, about 31 times the terrestrial reference value of 1.5×10^{-4}). Both the high content of organic matter and the elevated D/H ratios support a cometary origin of these ultracarbonaceous micrometeorites.

However, the existence of a radical distinction between asteroids and comets has been questioned in recent years. Comets that have orbits indistinguishable from those of Main Belt asteroids have been observed (Hsieh and Jewitt 2006). Very recently, water ice, previously supposed to be present only in comets, has been detected for the first time on the surface of an asteroid (Campins et al. 2010; Rivkin and Emery 2010). The study of comet Wild 2 samples, returned by the Stardust mission, showed that high temperature phases, as those present in meteorites, exist in cometary material, and that cometary and meteorite organic matter are quite similar (Brownlee et al. 2006; Sandford et al. 2006; Zolensky et al. 2006; Rotundi et al. 2008). Chondritic porous IDPs have reflectance spectra consistent with those of D- and P-type asteroids (Bradley et al. 1996), and spectra of hydrated, chondritic smooth IDPs are consistent with those of C-type asteroids (Bradley 2003). High ^{15}N enrichments, at the level measured in IDPs, have been observed also in samples usually considered of asteroidal origin: the CR and CH carbonaceous chondrites, where bulk ^{15}N enrichments have been observed (Krot et al. 2002); and the insoluble organic matter (IOM) extracted from carbonaceous chondrites (Busemann et al. 2007). Similarly, elevated D/H ratios have been measured in IOM of carbonaceous chondrites (Busemann et al. 2006; Remusat et al. 2006; Alexander et al. 2007, 2010). Even if no meteorite shows definitive evidence of a cometary origin, different studies proposed that CI carbonaceous chondrites, in many respects similar to the asteroidal CM and CR carbonaceous chondrites, originate from comets (Campins and Swindle 1998; Lodders and Osborne 1999; Gounelle et al. 2006, 2008). Also, recent results (Nesvorný et al. 2010) show that a large fraction of the micrometeorites that enter the Earth atmosphere originated from JFCs, implying that the collected carbonaceous micrometeorites represent both cometary and asteroidal samples.

Based on these observations, the idea of a continuum between carbonaceous asteroids and comets has been proposed (Gounelle et al. 2008; Gounelle 2011). This idea can explain why we do not see two clearly distinct classes of microxenoliths in howardites and H

chondrites, despite that our study in this article shows that howardites and H chondrite parent bodies should receive roughly equal proportion of cometary and asteroidal dust.

However, it is possible that the microxenoliths that we see in howardites and H chondrites are not representative of the current steady state of dust onto Main Belt asteroids, which was the basic assumption behind our work. Rubin and Bottke (2009) proposed that most microxenoliths have been accreted during specific events in the history of the asteroid belt, when the dust population was dominated by one source. For instance, the microxenoliths could have in vast majority a cometary origin if they have been accreted during the so-called Late Heavy Bombardment phase (about 3.9 Ga), presumably characterized by a much more intense flux of comets than at the current time (Gomes et al. 2005). Or the microxenoliths could have in vast majority an asteroidal origin if they have been accreted in the aftermath of the break-up of a big carbonaceous asteroid family. The fact that microxenoliths are very similar to the micrometeorites that fell on Earth in more recent times makes us think that the former are also representative of the dust distribution in the current steady state, rather than of the dust distribution during specific, sporadic events. If this is right, then the continuum of mineralogical and chemical properties within the microxenolith population argues in favor of a continuum between carbonaceous asteroids and comets.

Such a continuum might imply that the environment in which primordial asteroids formed in the asteroid belt was similar to that of the outer planetesimal disk, in the region of the giant planets and beyond, in which comets formed. However, it could also suggest that primordial asteroids did not form in the asteroid belt, but have been implanted into the belt from the outer planetesimal disk. Recent dynamical studies seem to support this idea. Levison et al. (2009) showed that during the Late Heavy Bombardment some planetesimals from the trans-Neptunian disk should have been implanted into the asteroid belt, and made a case that these implanted objects are the asteroids currently identified as P- and D-type. Morbidelli (2009) and Walsh et al. (2010) proposed that C-type asteroids have been captured from the region of the giant planets during the gas-disk phase, while the giant planets were growing and/or migrating. If all these dynamical studies are correct, then the continuum between primitive asteroids and comets is self-evident, as they come from basically the same parent reservoir.

CONCLUSIONS

In this article, we analyzed possible different sources for carbonaceous microxenoliths observed in howardites

and H chondrites. We performed numerical simulations to calculate the orbital evolution of micrometeoroids originated from JFCs and primordial asteroids (of spectral type C, D, and P) and their collision probability with targets represented by six Main Belt asteroids, proposed as the parent bodies of howardites and H chondrites. To quantify the micrometeoroid mass flux toward the target asteroids, we used recent estimations of the zodiacal cloud mass and of the relative contributions of asteroids and JFCs to it.

Our results show that two groups of carbonaceous microxenoliths, asteroidal and cometary, should be present among observed microxenoliths. However, these results do not indicate a clear prevalence of primordial asteroids or comets as source of microxenoliths. Instead, both populations of microxenoliths should be present on the considered asteroids (with the only exception of Koronis, which appears to receive more asteroidal than cometary micrometeoroids). This is somewhat in contrast with observations of microxenoliths in howardites and H chondrites: two different populations, clearly distinct by their composition, structure, and mineralogy, have never been observed. Indeed, differences among microxenoliths are present, such that it is possible to compare them with different groups of carbonaceous chondrites. However, just as for carbonaceous chondrites, such differences do not suggest that these microxenoliths derive from two groups of sharply different parent bodies.

Therefore, this work joins recent results in supporting the idea of an asteroids–comets continuum, i.e., that the differences in structure and composition between primordial asteroids and comets are less sharp than previously thought.

Acknowledgments—We want to thank the associate editor and the referees for their valuable comments. This work has been supported by the French Programme National de Planétologie (PNP).

Editorial Handling—Dr. Donald Brownlee

REFERENCES

- Alexander C. M. O'D., Fogel M., Yabuta H., and Cody G. D. 2007. The origin and evolution of chondrites recorded in the elemental and isotopic compositions of their macromolecular organic matter. *Geochimica et Cosmochimica Acta* 71:4380–4403.
- Alexander C. M. O'D., Newsome S. D., Fogel M. L., Nittler L. R., Busemann H., and Cody G. D. 2010. Deuterium enrichments in chondritic macromolecular material—Implications for the origin and evolution of organics, water and asteroids. *Geochimica et Cosmochimica Acta* 74:4417–4437.
- Babadzhanov P. B. and Kokhirova G. I. 2009. Densities and porosities of meteoroids. *Astronomy & Astrophysics* 495:353–358.

- Baer J., Chesley S., and Britt D. 2009. Asteroid masses V1.0, EAR-A-COMPIL-5-ASTMASS-V1.0 Online database: <http://sbn.psi.edu/pds/resource/astmass.html>.
- Balsiger H., Altwegg K., and Geiss J. 1995. D/H and $^{18}\text{O}/^{16}\text{O}$ ratio in the hydronium ion and in neutral water from in situ ion measurements in comet Halley. *Journal of Geophysical Research* 100:5827–5834.
- Binzel R. P. and Xu S. 1993. Chips off of asteroid 4 Vesta—Evidence for the parent body of basaltic achondrite meteorites. *Science* 260:186–191.
- Bischoff A., Scott E. R. D., Metzler K., and Goodrich C. A. 2006. Nature and origins of meteoritic breccias. In *Meteorites and the early solar system II*, edited by Lauretta D. S. and McSween H. Y. Tucson, Arizona: The University of Arizona Press. pp. 679–712.
- Bland P. A., Cintala M. J., Hörz F., and Cressey G. 2001. Survivability of meteorite projectiles—Results from impact experiments (abstract #1764). 32nd Lunar and Planetary Science Conference. CD-ROM.
- Bockelée-Morvan D., Gautier D., Lis D. C., Young K., Keene J., Phillips T., Owen T., Crovisier J., Goldsmith P. F., Bergin E. A., Despois D., and Wootten A. 1998. Deuterated water in comet C/1996 B2 (Hyakutake) and its implications for the origin of comets. *Icarus* 133:147–162.
- Bockelée-Morvan D., Biver N., Jehin E., Cochran A. L., Wiesemeyer H., Manfroid J., Hutsemékers D., Arpigny C., Boissier J., Cochran W., Colom P., Crovisier J., Milutinovic N., Moreno R., Prochaska J. X., Ramirez I., Schulz R., and Zucconi J.-M. 2008. Large excess of heavy nitrogen in both hydrogen cyanide and cyanogen from comet 17P/Holmes. *The Astrophysical Journal* 679:49–52.
- Borovička J. 2006. Physical and chemical properties of meteoroids as deduced from observations. In *Asteroids, comets, meteors*, vol. 229, edited by Lazzaro D., Ferraz-Mello S., and Fernandez J. A. Cambridge: Cambridge University Press. pp. 249–271.
- Borovička J., Spurný P., and Koten P. 2007. Atmospheric deceleration and light curves of Draconid meteors and implications for the structure of cometary dust. *Astronomy & Astrophysics* 473:661–672.
- Bottke W., Vokrouhlický D., Nesvorný D., and Shrubny L. 2010. (6) Hebe really is the H chondrite parent body (abstract #46.06). Proceedings, DPS meeting #42.
- Bradley J. P. 2003. Interplanetary dust particles. In *Meteorites, comets, and planets*, edited by Davis A. M. Treatise on Geochemistry, vol. 1. Heidelberg: Elsevier. pp. 689–711.
- Bradley J. P., Keller L. P., Brownlee D. E., and Thomas K. L. 1996. Reflectance spectra of interplanetary dust particles. *Meteoritics & Planetary Science* 31:394–402.
- Brearley A. J. 2006. The action of water. In *Meteorites and the early solar system*, edited by Lauretta D. S. and McSween H. Y. Tucson, Arizona: The University of Arizona Press. pp. 587–624.
- Briani G., Gounelle M., Bourot-Denise M., and Zolensky M. E. Forthcoming. Xenoliths and microxenoliths in H chondrites: Sampling the zodiacal cloud in the asteroid main belt. *Meteoritics & Planetary Science*.
- Brownlee D. E. 2003. Comets. In *Meteorites, comets, and planets*, edited by Davis A. M. Treatise on Geochemistry, vol. 1. Heidelberg: Elsevier. pp. 663–688.
- Brownlee D., Tsou P., Aléon J., Alexander C. M. O'D., Araki T., Bajt S., Baratta G. A., Bastien R., Bland P. A., Bleuet P., Bradley J. P., Brearley A., Brenker F., Brennan S., Bridges J. C., Browning N. D., Brucato J. R., Bullock E., Burchell M. J., Busemann H., Butterworth A., Chaussidon M., Chevront A., Chi M., Cintala M. J., Clark B. C., Clemett S. J., Cody G., Colangeli L., Cooper G., Cordier P., Daghlian C., Dai Z., D'Hendecourt L., Djouadi Z., Dominguez G., Duxbury T., Dworkin J. P., Ebel D. S., Economou T. E., Fakra S., Fairey S. A. J., Fallon S., Ferrini G., Ferroir T., Fleckenstein H., Floss C., Flynn G., Franchi I. A., Fries M., Gainsforth Z., Gallien J.-P., Genge M., Gilles M. K., Gillet P., Gilmour J., Glavin D. P., Gounelle M., Grady M. M., Graham G. A., Grant P. G., Green S. F., Grossemy F., Grossman L., Grossman J. N., Guan Y., Hagiya K., Harvey R., Heck P., Herzog G. F., Hoppe P., Hörz F., Huth J., Hutcheon I. D., Ignatyev K., Ishii H., Ito M., Jacob D., Jacobsen C., Jacobsen S., Jones S., Joswiak D., Jurewicz A., Kearsley A. T., Keller L. P., Khodja H., Kilcoyne A. L. D., Kissel J., Krot A., Langenhorst F., Lanzirotti A., Le L., Leshin L. A., Leitner J., Lemelle L., Leroux H., Liu M.-C., Luening K., Lyon I., MacPherson G., Marcus M. A., Marhas K., Marty B., Matrajt G., McKeegan K., Meibom A., Mennella V., Messenger K., Messenger S., Mikouchi T., Mostefaoui S., Nakamura T., Nakano T., Newville M., Nittler L. R., Ohnishi I., Ohsumi K., Okudaira K., Papanastassiou D. A., Palma R., Palumbo M. E., Pepin R. O., Perkins D., Perronnet M., Pianetta P., Rao W., Rietmeijer F. J. M., Robert F., Rost D., Rotundi A., Ryan R., Sandford S. A., Schwandt C. S., See T. H., Schlutter D., Sheffield-Parker J., Simionovici A., Simon S., Sitnitsky I., Snead C. J., Spencer M. K., Stadermann F. J., Steele A., Stephan T., Stroud R., Susini J., Sutton S. R., Suzuki Y., Taheri M., Taylor S., Teslich N., Tomeoka K., Tomioka N., Toppani A., Trigo-Rodríguez J. M., Troadec D., Tsuchiyama A., Tuzzolino A. J., Tyliczszak T., Uesugi K., Velbel M., Vellenga J., Vicenzi E., Vincze L., Warren J., Weber I., Weisberg M., Westphal A. J., Wirick S., Wooden D., Wopenka B., Wozniakiewicz P., Wright I., Yabuta H., Yano H., Young E. D., Zare R. N., Zega T., Ziegler K., Zimmerman L., Zinner E., and Zolensky M. E. 2006. Comet 81P/Wild 2 under a microscope. *Science* 314:1711–1716.
- Burbine T. H., McCoy T. J., Meibom A., Gladman B., and Keil K. 2002. Meteoritic parent bodies: Their number and identification. In *Asteroids III*, edited by Bottke W. F., Cellino A., Paolicchi P., and Binzel R. P. Tucson, Arizona: The University of Arizona Press. pp. 653–667.
- Bus S. J. and Binzel R. P. 2002. Phase II of the small main-belt asteroid spectroscopic survey. A featured-based taxonomy. *Icarus* 158:146–177.
- Bus S. J., Vilas F., and Barucci M. A. 2002. Visible-wavelength spectroscopy of asteroids. In *Asteroids III*, edited by Bottke W., Cellino A., Paolicchi P., and Binzel R. P. Tucson, Arizona: The University of Arizona Press. pp. 169–182.
- Busemann H., Young A. F., Alexander C. M. O'D., Hoppe P., Mukhopadhyay S., and Nittler L. R. 2006. Interstellar chemistry recorded in organic matter from primitive meteorites. *Science* 312:727–730.
- Busemann H., Alexander C. M. O'D., and Nittler L. R. 2007. Characterization of insoluble organic matter in primitive meteorites by microRaman spectroscopy. *Meteoritics & Planetary Science* 42:1387–1416.
- Campins H. and Swindle T. D. 1998. Expected characteristics of cometary meteorites. *Meteoritics & Planetary Science* 33:1201–1211.
- Campins H., Hargrove K., Pinilla-Alonso N., Howell E. S., Kelley M. S., Licandro J., Mothé-Diniz T., Fernández Y., and Ziffer J. 2010. Water ice and organics on the surface of the asteroid 24 Themis. *Nature* 464:1320–1321.

- Chappelou J. E. and Sharpton V. L. 2006. Atmospheric variations and meteorite production on Mars. *Icarus* 184:424–435.
- Cottin H., Gazeau M. C., and Raulin F. 1999. Cometary organic chemistry: A review from observations, numerical and experimental simulations. *Planetary and Space Science* 47:1141–1162.
- Dobrică E., Engrand C., Duprat J., Gounelle M., Leroux H., Quirico E., and Rouzaud J. N. 2009. Connection between micrometeorites and Wild 2 particles: From Antarctic snow to cometary ices. *Meteoritics & Planetary Science* 44:1643–1661.
- Drake M. J. 2001. The eucrite/Vesta story. *Meteoritics & Planetary Science* 36:501–513.
- Duprat J., Engrand C., Maurette M., Kurat G., Gounelle M., and Hammer C. 2007. Micrometeorites from central Antarctic snow: The CONCORDIA collection. *Advances in Space Research* 39:605–611.
- Duprat J., Dobrică E., Engrand C., Aléon J., Marrocchi Y., Mostefaoui S., Meibom A., Leroux H., Rouzaud J.-N., Gounelle M., and Robert F. 2010. Extreme deuterium excesses in ultracarbonaceous micrometeorites from central Antarctic snow. *Science* 328:742–745.
- Eberhardt P., Reber M., Krankowsky D., and Hodges R. R. 1995. The D/H and $^{18}\text{O}/^{16}\text{O}$ ratios in water from comet P/Halley. *Astronomy & Astrophysics* 302:301–316.
- Engrand C. and Maurette M. 1998. Carbonaceous micrometeorites from Antarctica. *Meteoritics & Planetary Science* 33:565–580.
- Farinella P., Froeschle C., and Gonczi R. 1993. Meteorites from the asteroid 6 Hebe. *Celestial Mechanics and Dynamical Astronomy* 56:287–305.
- Floss C., Stadermann F. J., Bradley J. P., Dai Z. R., Bajt S., Graham G., and Lea A. S. 2006. Identification of isotopically primitive interplanetary dust particles: A NanoSIMS isotopic imaging study. *Geochimica et Cosmochimica Acta* 70:2371–2399.
- Flynn G. J. 1995. Atmospheric entry heating of large interplanetary dust particles. *Meteoritics* 30:504.
- Flynn G. J., Durda D. D., Sandel L. E., Kreft J. W., and Strait M. M. 2009. Dust production from the hypervelocity impact disruption of the Murchison hydrous CM2 meteorite: Implications for the disruption of hydrous asteroids and the production of interplanetary dust. *Planetary and Space Science* 57:119–126.
- Gaffey M. J. and Gilbert S. L. 1998. Asteroid 6 Hebe: The probable parent body of the H-type ordinary chondrites and the IIE iron meteorites. *Meteoritics & Planetary Science* 33:1281–1295.
- Genge M. J. 2006. Ordinary chondrite micrometeorites from the Koronis asteroids (abstract #1759). 37th Lunar and Planetary Science Conference. CD-ROM.
- Genge M. J., Grady M. M., and Hutchison R. 1997. The textures and compositions of fine-grained Antarctic micrometeorites—Implications for comparisons with meteorites. *Geochimica et Cosmochimica Acta* 61:5149.
- Genge M., Engrand C., Gounelle M., and Taylor S. 2008. The classification of micrometeorites. *Meteoritics & Planetary Science* 43:497–515.
- Gomes R., Levison H. F., Tsiganis K., and Morbidelli A. 2005. Origin of the cataclysmic Late Heavy Bombardment period of the terrestrial planets. *Nature* 435:466–469.
- Gounelle M. 2011. The asteroid-comet continuum: In search of lost primitivity. *Elements* 7:29–34.
- Gounelle M., Zolensky M. E., Liou J.-C., Bland P. A., and Alard O. 2003. Mineralogy of carbonaceous chondritic microclasts in howardites: Identification of C2 fossil micrometeorites. *Geochimica et Cosmochimica Acta* 67:507–527.
- Gounelle M., Engrand C., Alard O., Bland P. A., Zolensky M. E., Russell S. S., and Duprat J. 2005. Hydrogen isotopic composition of water from fossil micrometeorites in howardites. *Geochimica et Cosmochimica Acta* 69:3431–3443.
- Gounelle M., Spurný P., and Bland P. A. 2006. The orbit and atmospheric trajectory of the Orgueil meteorite from historical records. *Meteoritics & Planetary Science* 41:135–150.
- Gounelle M., Morbidelli A., Bland P. A., Spurný P., Young E. D., and Sephton M. 2008. Meteorites from the outer solar system? In *The solar system beyond Neptune*, edited by Barucci M. A., Boehnhardt H., Cruikshank D. P., and Morbidelli A. Tucson, Arizona: The University of Arizona Press. pp. 525–541.
- Gounelle M., Chaussidon M., Morbidelli A., Barrat J. A., Engrand C., Zolensky M. E., and McKeegan K. D. 2009. A unique basaltic micrometeorite expands the inventory of solar system planetary crusts. *Proceedings of the National Academy of Sciences* 106:6904–6909.
- Greshake A., Krot A. N., Meibom A., Weisberg M. K., Zolensky M. E., and Keil K. 2002. Heavily hydrated lithic clasts in CH chondrites and the related, metal-rich chondrites Queen Alexandra Range 94411 and Hammadah al Hamra 237. *Meteoritics & Planetary Science* 37:281–293.
- Grün E., Zook H. A., Fechtig H., and Giese R. H. 1985. Collisional balance of meteoritic complex. *Icarus* 62:244–272.
- Gustafson B. A. S. 1994. Physics of zodiacal dust. *Annual Review of Earth and Planetary Sciences* 22:553–595.
- Hiroi T., Pieters C. M., and Zolensky M. E. 1993a. Comparison of reflectance spectra of C asteroids and unique C chondrites Y86720, Y82162, and B7904 (abstract). 24th Lunar and Planetary Science Conference. pp. 659–660.
- Hiroi T., Pieters C. M., Zolensky M. E., and Lipschutz M. E. 1993b. Evidence of thermal metamorphism on the C, G, B and F asteroids. *Science* 261:1016–1018.
- Hsieh H. H. and Jewitt D. 2006. A population of comets in the main asteroid belt. *Science* 312:561–563.
- Huss G. R., Rubin A. E., and Grossman J. N. 2006. Thermal metamorphism in chondrites. In *Meteorites and the early solar system II*, edited by Lauretta D. S. and McSween H. Y. Tucson, Arizona: The University of Arizona Press. pp. 567–586.
- Johnson T. V. and Fanale F. B. 1973. Optical properties of carbonaceous chondrites and their relationship to asteroids. *Journal of Geophysical Research* 78:8507–8515.
- Krot A., Meibom A., Weisberg M., and Keil K. 2002. The CR chondrite clan: Implications for early solar system processes. *Meteoritics & Planetary Science* 37:1451–1490.
- Leinert C., Roser S., and Buitrago J. 1983. How to maintain the spatial distribution of interplanetary dust. *Astronomy & Astrophysics* 118:345–357.
- Levison H. F. and Duncan M. J. 1997. From the Kuiper Belt to Jupiter-family comets: The spatial distribution of ecliptic comets. *Icarus* 127:13–32.
- Levison H. F., Bottke W. F., Gounelle M., Morbidelli A., Nesvorný D., and Tsiganis K. 2009. Contamination of the asteroid belt by primordial trans-Neptunian objects. *Nature* 460:364–366.
- Lipschutz M. E., Gaffey M. J., and Pellas P. 1989. Meteoritic parent bodies—Nature, number, size and relation to present-day asteroids. In *Asteroids II*, edited by Binzel R.

- P., Gehrels T., and Shapely Matthews M. Tucson, Arizona: University of Arizona Press. pp. 740–777.
- Lodders K. and Osborne R. 1999. Perspectives on the comet-asteroid-meteorite link. *Space Science Reviews* 90:289–297.
- Love S. G. and Brownlee D. E. 1993. A direct measurement of the terrestrial mass accretion rate of cosmic dust. *Science* 262:550–553.
- Manfroid J., Jehin E., Hutsemékers D., Cochran A. L., Zucconi J.-M., Arpigny C., Schulz R., and Stuwe J. A. 2005. Isotopic abundance of nitrogen and carbon in distant comets. *Astronomy & Astrophysics* 432:5–8.
- Maurette M., Duprat J., Engrand C., Gounelle M., Kurat G., Matrajt G., and Toppani A. 2000. Accretion of neon, organics, CO₂, nitrogen and water from large interplanetary dust particles on the early Earth. *Planetary and Space Science* 48:1117–1137.
- Meibom A. and Clark B. E. 1999. Evidence for the insignificance of ordinary chondritic material in the asteroid belt. *Meteoritics & Planetary Science* 34:7–24.
- Meier R., Owen T. C., Matthews H. E., Jewitt D. C., Bockelée-Morvan D., Biver N., Crovisier J., and Gautier D. 1998. A determination of the HDO/H₂O ratio in comet C/1995 O1 (Hale-Bopp). *Science* 279:842–844.
- Meier M. M. M., Schmitz B., Baur H., and Wieler R. 2010. Noble gases in individual L chondritic micrometeorites preserved in Ordovician limestone. *Earth and Planetary Science Letters* 290:54–63.
- Migliorini F., Manara A., Scaltriti F., Farinella P., Cellino A., and di Martino M. 1997. Surface properties of (6) Hebe: A possible parent body of ordinary chondrites. *Icarus* 128:104–113.
- Morbidelli A. 2009. Where do meteorites ultimately come from? (abstract #5450). 72nd Annual Meteoritical Society Meeting. *Meteoritics & Planetary Science* 44.
- Nakashima D., Nakamura T., and Noguchi T. 2003. Formation history of CI-like phyllosilicate-rich clasts in the Tsukuba meteorite inferred from mineralogy and noble gas signatures. *Earth and Planetary Science Letters* 212:321–336.
- Nesvorný D., Vokrouhlický D., Bottke W. F., and Sykes M. 2006. Physical properties of asteroid dust bands and their sources. *Icarus* 181:107–144.
- Nesvorný D., Jenniskens P., Levison H. F., Bottke W. F., Vokrouhlický D., and Gounelle M. 2010. Cometary origin of the zodiacal cloud and carbonaceous micrometeorites. *The Astrophysical Journal* 713:816–836.
- Remusat L., Palhol F., Robert F., Derenne S., and France-Lanord C. 2006. Enrichment of deuterium in insoluble organic matter from primitive meteorites: A solar system origin? *Earth and Planetary Science Letters* 243:15–25.
- Rivkin A. S. and Emery J. P. 2010. Detection of ice and organics on an asteroidal surface. *Nature* 464:1322–1323.
- Rotundi A., Baratta G. A., Borg J., Brucato J. R., Busemann H., Colangeli L., D'Hendecourt L., Djouadi Z., Ferrini G., Franchi I. A., Fries M., Grossemy F., Keller L. P., Mennella V., Nakamura K., Nittler L. R., Palumbo M. E., Sandford S. A., Steele A., and Wopenka B. 2008. Combined micro-Raman, micro-infrared, and field emission scanning electron microscope analyses of comet 81P/Wild 2 particles collected by Stardust. *Meteoritics & Planetary Science* 43:367–397.
- Rubin A. E. and Bottke W. F. 2009. On the origin of shocked and unshocked CM clast in H-chondrite regolith breccias. *Meteoritics & Planetary Science* 44:701–724.
- Sandford S. A., Aléon J., Alexander C. M. O. D., Araki T., Bajt S., Baratta G. A., Borg J., Bradley J. P., Brownlee D. E., Brucato J. R., Burchell M. J., Busemann H., Butterworth A., Clemett S. J., Cody G., Colangeli L., Cooper G., D'Hendecourt L., Djouadi Z., Dworkin J. P., Ferrini G., Fleckenstein H., Flynn G. J., Franchi I. A., Fries M., Gilles M. K., Glavin D. P., Gounelle M., Grossemy F., Jacobsen C., Keller L. P., Kilcoyne A. L. D., Leitner J., Matrajt G., Meibom A., Mennella V., Mostefaoui S., Nittler L. R., Palumbo M. E., Papanastassiou D. A., Robert F., Rotundi A., Snead C. J., Spencer M. K., Stadermann F. J., Steele A., Stephan T., Tsou P., Tyliczszak T., Westphal A. J., Wirick S., Wopenka B., Yabuta H., Zare R. N., and Zolensky M. E. 2006. Organics captured from comet 81P/Wild 2 by the Stardust spacecraft. *Science* 314:1720–1724.
- Taylor S. and Brownlee D. E. 1991. Cosmic spherules in the geologic record. *Meteoritics* 26:203–211.
- Tholen D. J. 1989. Asteroid taxonomic classification. In *Asteroids II*, edited by Binzel R. P., Gehrels T., and Shapely Matthews M. Tucson, Arizona: The University of Arizona Press. pp. 1139–1150.
- Tomeoka K., Kiriyama K., Nakamura K., Yamahana Y., and Sekine T. 2003. Interplanetary dust from the explosive dispersal of hydrated asteroids by impacts. *Nature* 423:60–62.
- Vilas F. and Gaffey M. J. 1989. Phyllosilicate absorption features in main-belt and outer asteroid reflectance spectra. *Science* 246:790–792.
- Walsh K. J., Morbidelli A., Raymond S. N., O'Brien D. P., and Mandell A. 2010. Origin of the asteroid belt and Mars' small mass (abstract #4.02). Proceedings, DPS meeting #42.
- Wetherill G. W. 1967. Collisions in the asteroid belt. *Journal of Geophysical Research* 72:2429–2444.
- Wilkening L. L. 1977. Meteorites in meteorites—Evidence for mixing among the asteroids. In *Comets, asteroids, meteorites: Interrelations, evolution and origins*. IAU Colloquium 39. Toledo, Ohio: University of Toledo. pp. 389–395.
- Willman M. and Jedicke R. 2011. Asteroid age distribution determined by space weathering and collisional evolution models. *Icarus* 211:504–510.
- Zolensky M. E., Weisberg M. K., Buchanen P. C., and Mittlefehldt D. W. 1996. Mineralogy of carbonaceous chondrite clasts in HED achondrites and the Moon. *Meteoritics & Planetary Science* 31:518–537.
- Zolensky M. E., Zega T. J., Yano H., Wirick S., Westphal A. J., Weisberg M. K., Weber I., Warren J. L., Velbel M. A., Tsuchiyama A., Tsou P., Toppani A., Tomioka N., Tomeoka K., Teslich N., Taheri M., Susini J., Stroud R., Stephan T., Stadermann F. J., Snead C. J., Simon S. B., Simionovici A., See T. H., Robert F., Rietmeijer F. J. M., Rao W., Perronnet M. C., Papanastassiou D. A., Okudaira K., Ohsumi K., Ohnishi I., Nakamura-Messenger K., Nakamura T., Mostefaoui S., Mikouchi T., Meibom A., Matrajt G., Marcus M. A., Leroux H., Lemelle L., Le L., Lanzirrotti A., Langenhorst F., Krot A. N., Keller L. P., Kearsley A. T., Joswiak D., Jacob D., Ishii H., Harvey R., Hagiya K., Grossman L., Grossman J. N., Graham G. A., Gounelle M., Gillet P., Genge M. J., Flynn G., Ferroir T., Fallon S., Ebel D. S., Dai Z. R., Cordier P., Clark B., Chi M., Butterworth A. L., Brownlee D. E., Bridges J. C., Brennan S., Brearley A., Bradley J. P., Bleuet P., Bland P. A., and Bastien R. 2006. Mineralogy and petrology of comet 81P/Wild 2 nucleus samples. *Science* 314:1735–1739.

APPENDIX

The cometary to asteroidal ratio of micrometeoroid flux φ is calculated as

$$\varphi = \frac{p_{\text{coll}}^{\text{JFC}}}{p_{\text{coll}}^{\text{AST}}} \times R = \text{PR}, \quad (\text{A1})$$

where $p_{\text{coll}}^{\text{JFC}}$ and $p_{\text{coll}}^{\text{AST}}$ are the mean probability of collision for asteroidal and cometary micrometeoroids, respectively, and R is the cometary to asteroidal ratio of micrometeoroid mass between 2 and 4 AU from the Sun.

The value for R is derived from estimates of Nesvorný et al. (2010) and is referred to particles with diameter $D = 200 \mu\text{m}$ and density $\rho = 2 \text{ g cm}^{-3}$. Therefore, we take as the best value of p_{coll} those obtained considering micrometeoroids with these properties. For each target asteroid, the value of the uncertainty Δp_{coll} is estimated taking into account both the uncertainty due to our numerical simulations and that due to the fact that micrometeoroids with different physical properties (in particular size and density) follow different orbital evolutions. The error due to our numerical simulations is estimated from simulations performed for micrometeoroid populations that have equal size and density (diameter = $200 \mu\text{m}$, density = 2 g cm^{-3}) and the same initial values of the orbital parameters a (semimajor axis), e (eccentricity), i (inclination), ω (argument of perihelion), and Ω (longitude of the ascending node), but different initial mean anomalies M (i.e., changing the initial positions of micrometeoroids on their orbits). Starting from the results of these simulations, we estimate the relative error on the collision probability as

$$\frac{\Delta p_{\text{coll}}^{\text{NUM}}}{p_{\text{coll}}} = \sqrt{\frac{1}{N_{\text{asteroids}}} \sum_{i=1}^6 \left(\frac{p_{\text{or}_M}^i - p_{\text{new}_M}^i}{p_{\text{or}_M}^i} \right)^2}, \quad (\text{A2})$$

where $N_{\text{asteroids}}$ is the total number of target asteroids (here equal to 6, given the asteroids that we considered as targets), $p_{\text{or}_M}^i$ is the micrometeoroid collision probability with the i th target asteroid calculated using results of the simulations with the original values of M , and $p_{\text{new}_M}^i$ is the micrometeoroid collision probability with the i th target asteroid calculated using results of the simulations with the new values of M . With this procedure the collision probability relative error, for both asteroidal and JFC micrometeoroids, is approximately 3%. To evaluate the error due to the different orbital evolution of micrometeoroids with different physical properties, we use the difference between the collision

probability of $D = 200 \mu\text{m}$ micrometeoroids and the collision probability of $D = 100 \mu\text{m}$ micrometeoroids; in other words:

$$\Delta p_{\text{coll}}^{\text{PHYS}} = |p_{\text{coll}}(200\mu\text{m}) - p_{\text{coll}}(100\mu\text{m})|. \quad (\text{A3})$$

The total error on the mean collision probability, for both asteroidal and cometary micrometeoroids, is then obtained as

$$\Delta p_{\text{coll}} = \sqrt{(\Delta p_{\text{coll}}^{\text{NUM}})^2 + (\Delta p_{\text{coll}}^{\text{PHYS}})^2} \quad (\text{A4})$$

and consequently the relative error on $P = p_{\text{coll}}^{\text{JFC}}/p_{\text{coll}}^{\text{AST}}$ is

$$\frac{\Delta P}{P} = \frac{\Delta p_{\text{coll}}^{\text{JFC}}}{p_{\text{coll}}^{\text{JFC}}} + \frac{\Delta p_{\text{coll}}^{\text{AST}}}{p_{\text{coll}}^{\text{AST}}}. \quad (\text{A5})$$

For the cometary to asteroidal mass ratio between 2 and 4 AU, Nesvorný et al. (2010) indicate that their mass estimations have an uncertainty of a factor 2. Assuming that the errors on the masses of asteroidal and cometary dusts are uncorrelated and that both are of a factor of 2 (which is probably a pessimistic assumption), the value of R can be as large as four times or as little as one-fourth of the reference value that we used (34). Therefore, the cometary to asteroidal ratio of micrometeoroid flux φ comprised between

$$\varphi_{\text{max}} = (P + \Delta P) \times 4R \quad \text{and} \quad \varphi_{\text{min}} = (P - \Delta P) \times \frac{1}{4}R. \quad (\text{A6})$$

The velocity v_{coll} of collisions between micrometeoroids and each target asteroid is estimated taking into account the gravitational focusing of the target. Therefore,

$$v_{\text{coll}} = \sqrt{v_{\infty}^2 + v_{\text{esc}}^2} \quad (\text{A7})$$

with v_{∞} is the micrometeoroid velocity on its orbit, calculated by the `swift_rmvs3_pr` code, and v_{esc} is the target asteroid escape velocity. The escape velocities for the six asteroids selected as targets are reported in Table A1, along with the values of radius and mass used to calculate v_{esc} . The error on v_{coll} reported in Table 2 is estimated as

$$\Delta v_{\text{coll}} = \frac{1}{v_{\text{coll}}} (v_{\infty} \Delta v_{\infty} + v_{\text{esc}} \Delta v_{\text{esc}}), \quad (\text{A8})$$

where the error Δv_{∞} is calculated in the same way described above for Δp_{coll} .

Table A1. Physical properties of the six asteroids selected as targets in our simulations.

Asteroid	Radius ^a (km)	Mass ^b ($\times 10^{18}$ kg)	Escape velocity (m s^{-1})
4 Vesta	261 ± 5	266 ± 8	369 ± 5
6 Hebe	93 ± 1	13 ± 2	139 ± 12
8 Flora	81 ± 12	8 ± 0.9	119 ± 11
15 Eunomia	134 ± 8	26 ± 3	160 ± 10
158 Koronis	35 ± 1	0.05 ± 0.006	19 ± 1
170 Maria	44 ± 1	0.09 ± 0.006	23 ± 1

^aData of asteroid dimensions for Vesta, Hebe, Flora, and Eunomia are from Baer et al. (2009) and references therein. The value reported here is the radius of a sphere equivalent in volume to the ellipsoid that has the axes reported in Baer et al. (2009). For Koronis and Maria, the radius is that reported in the JPL Small Body Database.

^bData of asteroid masses for Vesta, Hebe, Flora, and Eunomia are from Baer et al. (2009) and references therein. For Koronis and Maria, the mass is calculated assuming a density of 2 g cm^{-3} .